Supporting Information

Synthesis of bis(2-ethylhexyl) phosphate modified carbon quantum dots for enhanced oil-based lubrication

Bin Zhao [a], Meng Zhang [b], Beibei Zhang [c], Zihao Mou [a], Weiwei Tang [d], Zhijun Wang [a, *], Baogang Wang [b, *]

[a] Institute for Advanced Study, Chengdu University, Chengdu 610106, P. R. China.

[b] College of Chemistry and Chemical Engineering, Southwest Petroleum University, Chengdu 610500, P. R. China.

[c] Institute of Fundamental and Frontier Sciences, University of Electronic Science and Technology of China, Chengdu 610054, P. R. China.

[d] School of Biological and Chemical Engineering, Panzhihua University, Panzhihua 617000, P. R. China.

Corresponding authors: Zhijun Wang, wangzhijun@cdu.edu.cn

Baogang Wang, bgwang@swpu.edu.cn

1. Supplemental Figures

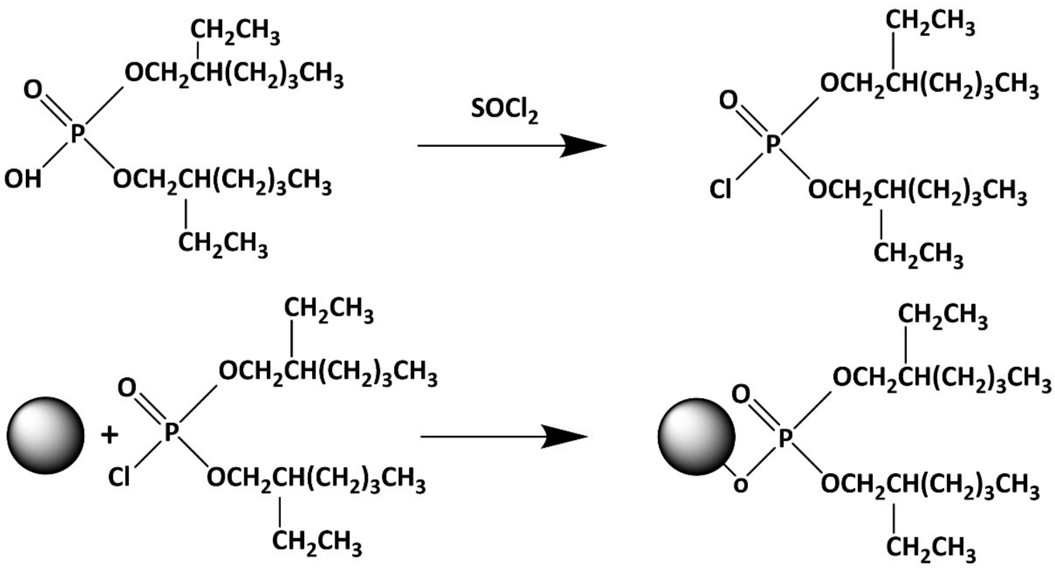

Schematic S1 The preparation pathway for CQDs-D_2EHPA.

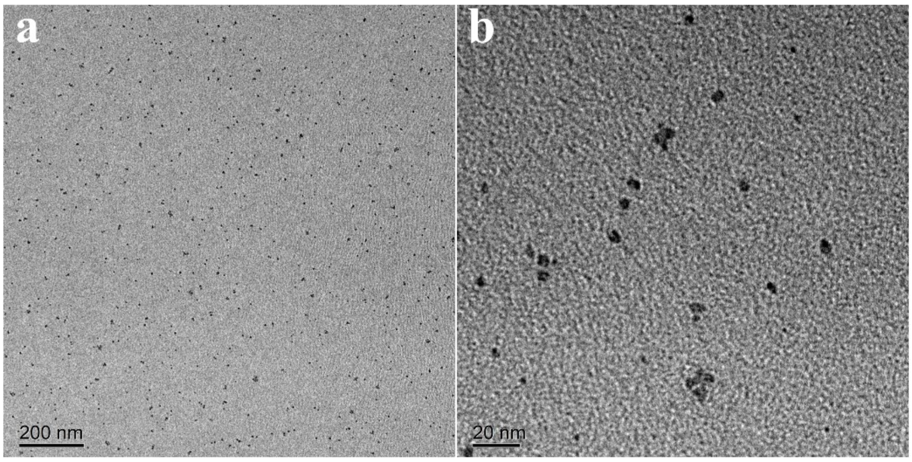

Figure S1 The typical TEM images of the prepared CQDs-D_2EHPA.

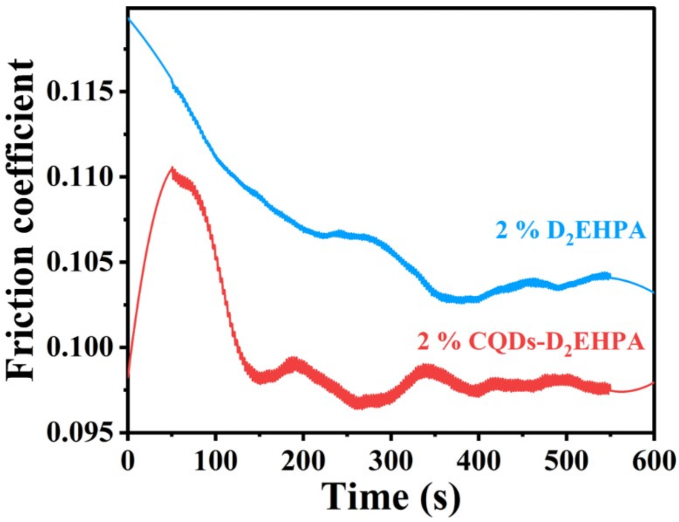

Figure S2 The friction coefficient curves for 2% CQDs-D_2EHPA and 2% D_2EHPA lubricant.

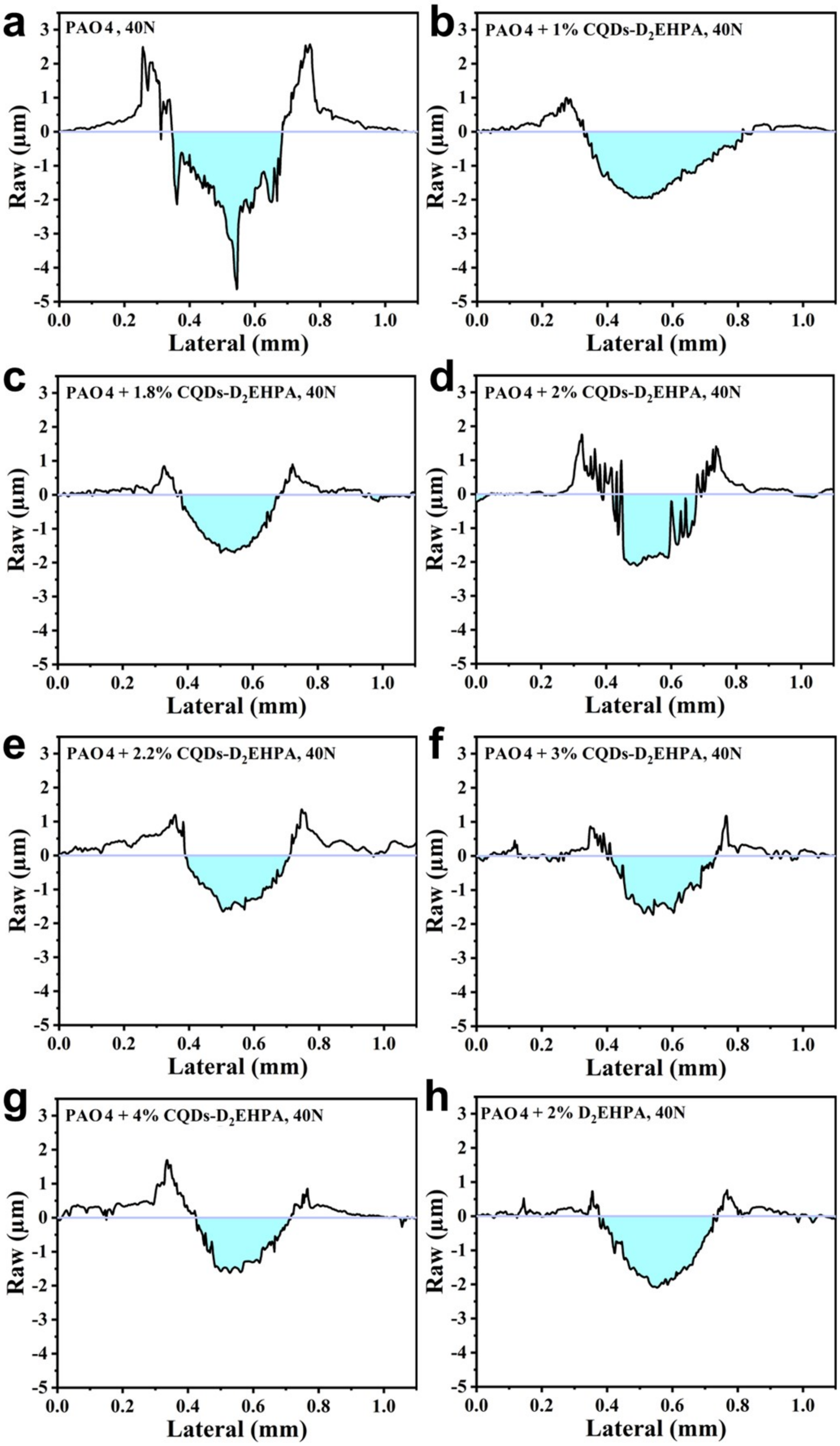

Figure S3 The cross-sectional views of the wear tracks corresponding to different additive concentrations of CQDs-D_2EHPA lubricant.

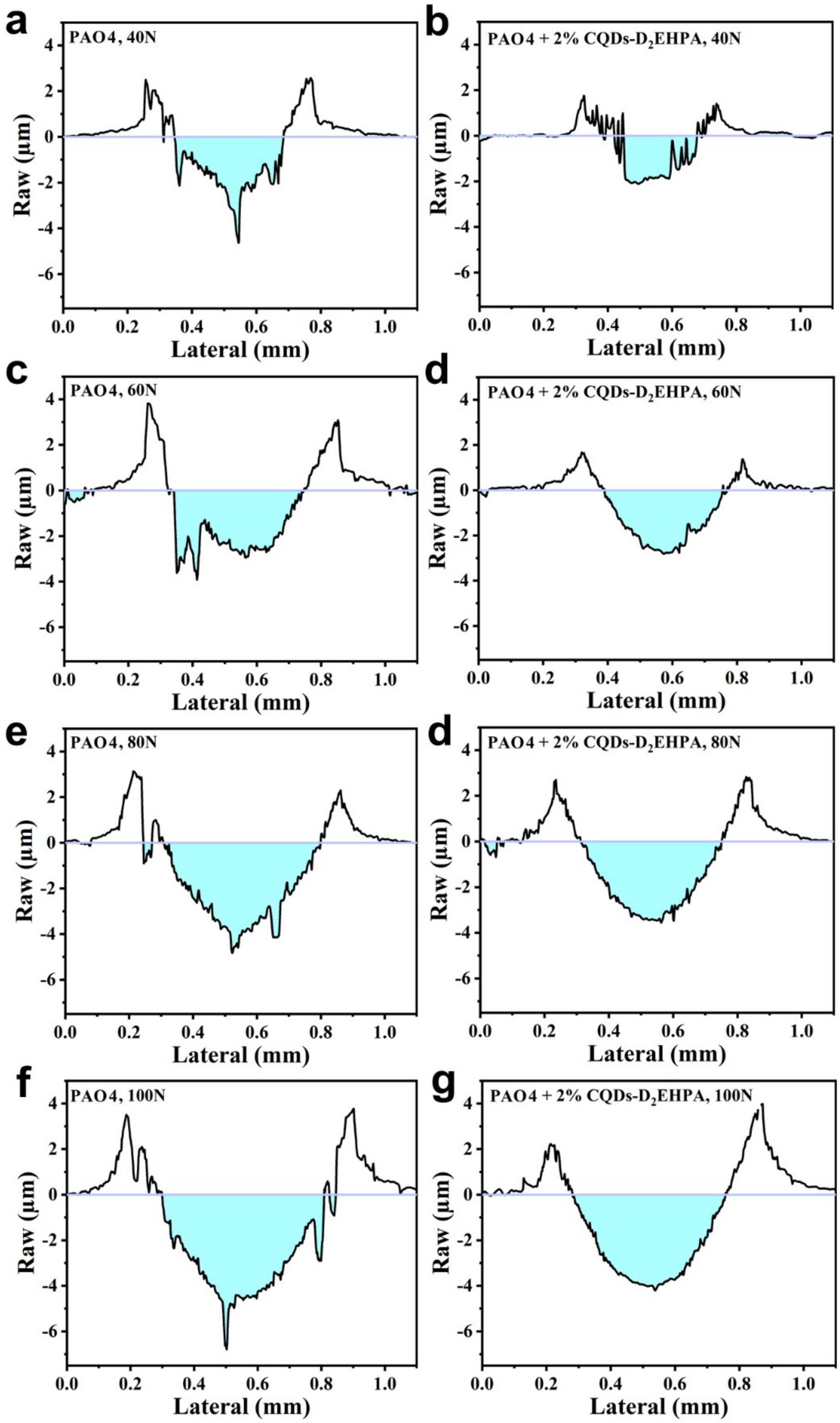

Figure S4 The cross-sectional views of the wear tracks corresponding to different load with 2% CQDs-D_2EHPA lubricant.

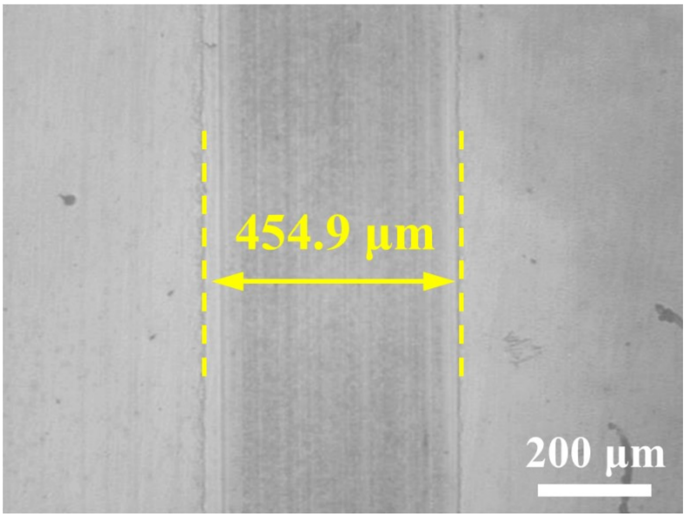

Figure S5 The typical SEM image of the wear tracks corresponding to 2% D_2EHPA lubricant.

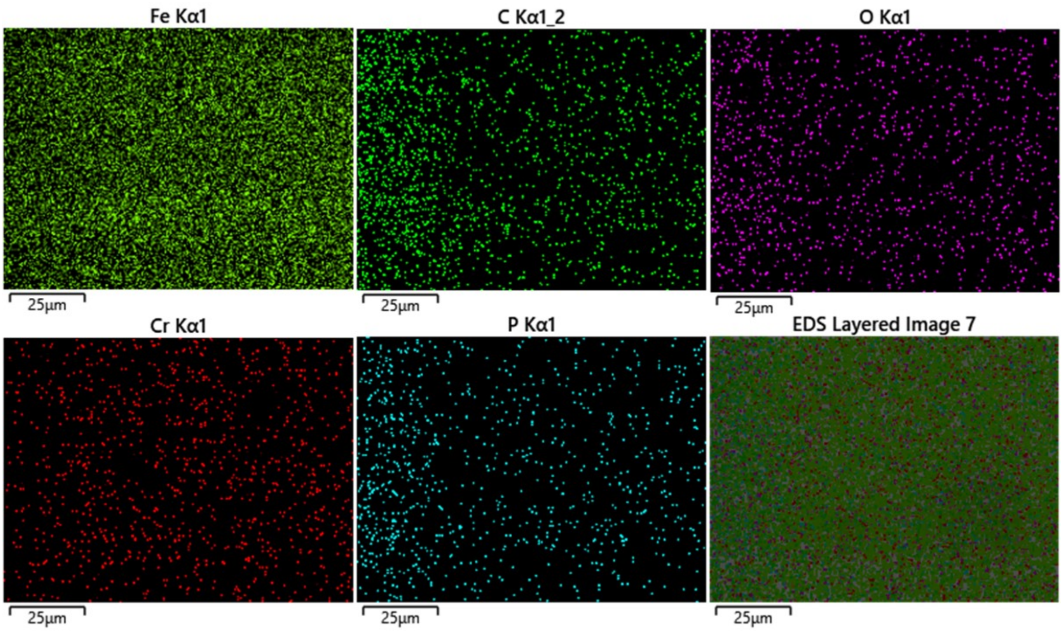

Figure S6 The EDS mapping results of the wear tracks corresponding to 2% D_2EHPA lubricant.

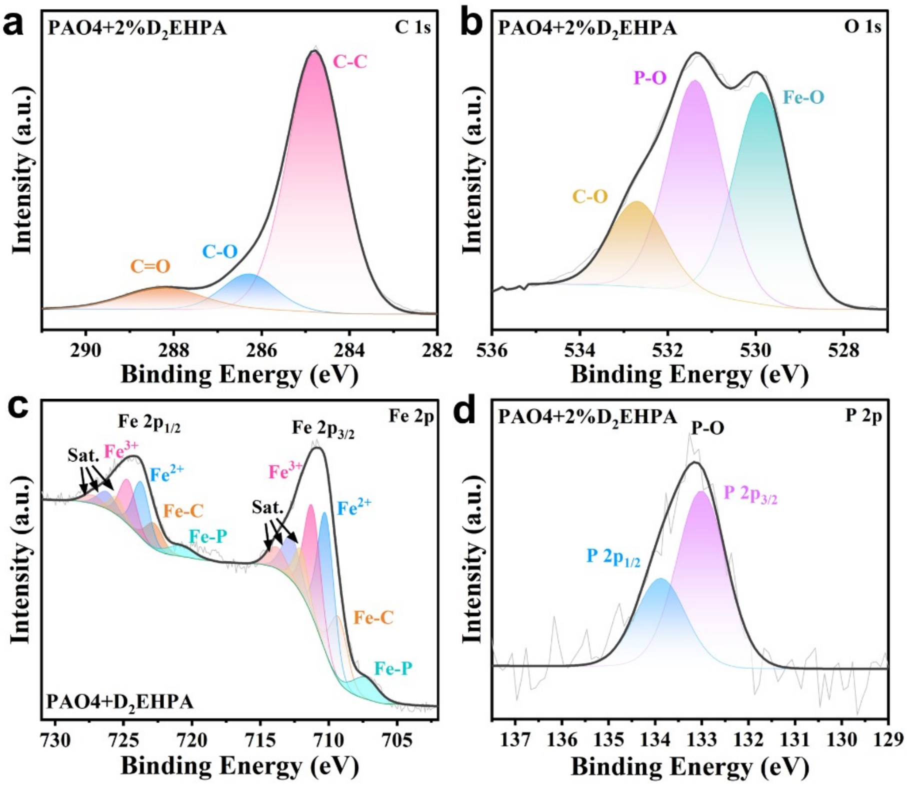

Figure S7 The high-resolution XPS spectrum of the wear tracks corresponding to 2% D_2EHPA lubricant.

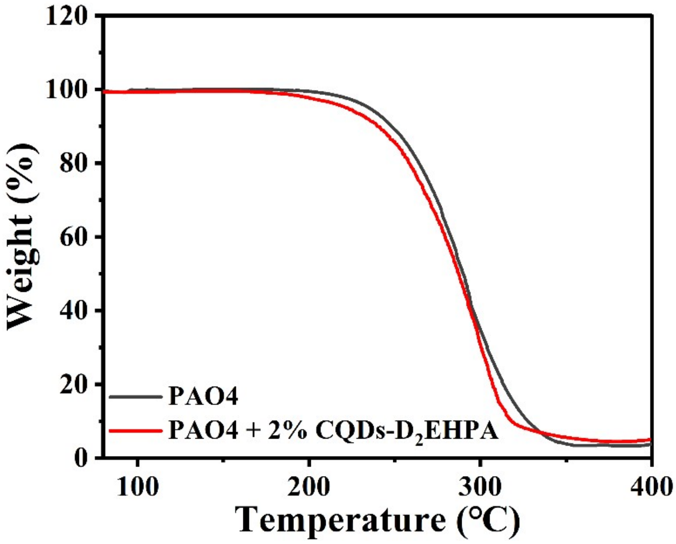

Figure S8 The TGA curves of PAO4 and PAO4 with 2% CQDs-D_2EHPA measured under Ar atmosphere with a heating rate of 10 °C/min.

As shown in Figure S8, the TGA curve of PAO4 with CQDs-D_2EHPA exhibits a noticeable mass loss between 200 °C and 350 °C, which is generally consistent with the behavior of the pristine PAO4. A slightly more pronounced mass loss is observed around 200 °C, followed by a marginally higher residual mass at 400 °C. These subtle differences align well with the thermal decomposition characteristics of CQDs-D_2EHPA itself.

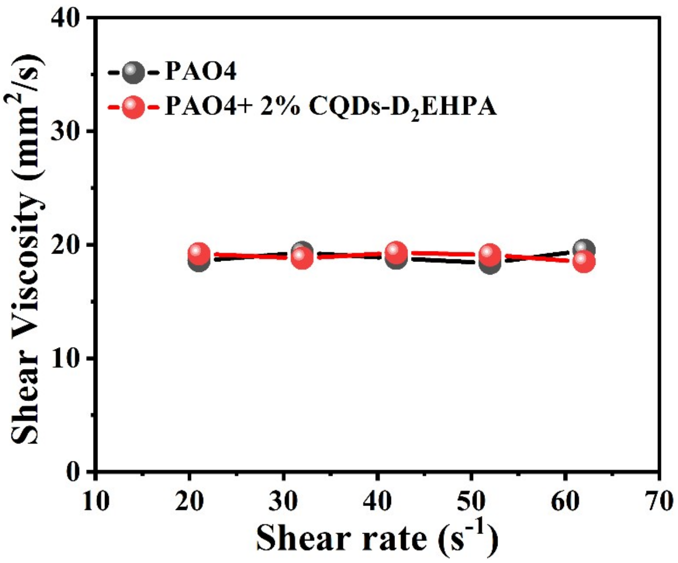

Figure S9 The shear viscosity at 30 ℃ of PAO4 with or without 2% CQDs-D_2EHPA under different shear rate.

The viscosity results (Figure S9) indicate that the kinematic viscosity of the lubricant remains nearly unchanged under different shear rates, consistent with the Newtonian fluid behavior expected for PAO4, and the addition of CQDs-D_2EHPA does not significantly alter the viscosity profile.

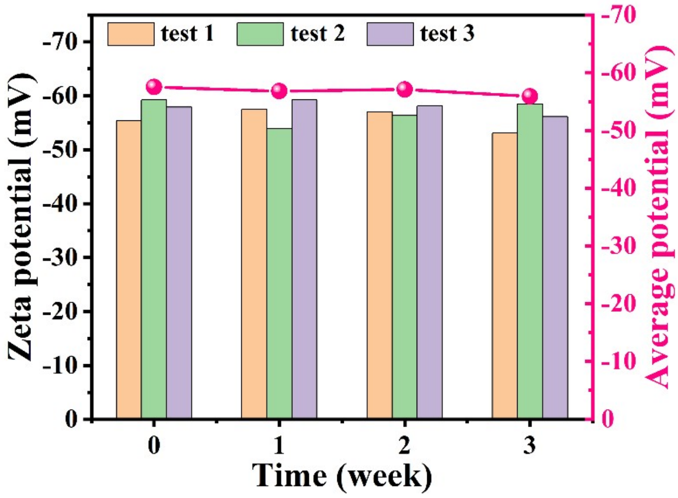

Figure S10 The zeta potential of PAO4 with 2% CQDs-D_2EHPA stored for different week.

Figure S10 presents the zeta potential data of the 2% CQDs-D_2EHPA dispersion in PAO4, stored at room temperature over three weeks. The freshly prepared dispersion exhibited a zeta potential of -57.5 mV, suggesting good initial stability. Importantly, no significant decrease in the zeta potential was observed throughout the three-week period, further attesting to the excellent dispersion stability of CQDs-D_2EHPA in PAO4.

2. *Supplemental Tables*

Table S1 The EDS analysis results of wear tracks corresponding to different lubricants.

Lubricant	**Fe wt%**	**Cr wt%**	**C wt%**	**O wt%**	**P wt%**
PAO4	80.21	1.46	15.71	2.63	--
PAO4+D_2EHPA	79.77	1.62	15.82	2.79	--
PAO4+CQDs-D_2EHPA	71.82	1.42	23.62	2.57	0.56

Table S2 Elemental composition of wear scars corresponding to different lubricants calculated from XPS results.

Lubricant	**Fe at%**	**C at%**	**O at%**	**P at%**
PAO4	0.75	79.63	19.62	--
PAO4+D_2EHPA	1.05	66.29	31.03	1.63
PAO4+CQDs-D_2EHPA	1.94	67.21	24.23	6.61